Journal of Neuroscience Methods xxx (2012) xxx–xxx

Contents lists available at SciVerse ScienceDirect

Journal of Neuroscience Methods

journal homepage: www.elsevier.com/locate/jneumeth

Computational Neuroscience

Anatomo-clinical atlases correlate clinical data and electrode contact coordinates: Application to subthalamic deep brain stimulation

Florent Lalys[a,b,*], Claire Haegelen[a,b,c], Maroua Mehri[a,b], Sophie Drapier[d], Marc Vérin[d], Pierre Jannin[a,b]

[a] MediCIS, INSERM, LTSI U1099, Faculté de Médecine CS 34317, F-35043 Rennes Cedex, France
[b] University of Rennes I, F-35042 Rennes, France
[c] Department of Neurosurgery, Pontchaillou University Hospital, F-35043 Rennes, France
[d] Department of Neurology, Pontchaillou University Hospital, F-35043 Rennes, France

HIGHLIGHTS

- Creation of anatomo-clinical atlases for SubThalamic Deep Brain Stimulation.
- Atlases enable extraction of representative clusters to determine the optimum site.
- Atlases help acquire a better understanding of functional mapping in deep structures.

GRAPHICAL ABSTRACT

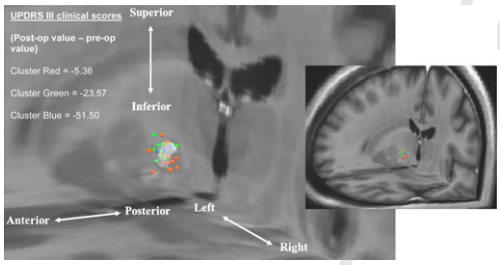

ARTICLE INFO

Article history:
Received 28 August 2012
Received in revised form 31 October 2012
Accepted 2 November 2012

Keywords:
Deep brain stimulation
Parkinson disease
Anatomo-clinical atlas
Medical imaging

ABSTRACT

For patients suffering from Parkinson's disease with severe movement disorders, functional surgery may be required when medical therapy is not effective. In Deep Brain Stimulation (DBS), electrodes are implanted within the brain to stimulate deep structures such as SubThalamic Nucleus (STN). The quality of patient surgical outcome is generally related to the accuracy of nucleus targeting during surgery. In this paper, we focused on identifying optimum sites for STN DBS by studying symptomatic motor improvement along with neuropsychological side effects. We described successive steps for constructing digital atlases gathering patient's location of electrode contacts automatically segmented from postoperative images, and clinical scores. Three motor and five neuropsychological scores were included in the study. Correlations with active contact locations were carried out using an adapted hierarchical ascendant classification. Such analysis enabled the extraction of representative clusters to determine the optimum site for therapeutic STN DBS. For each clinical score, we built an anatomo-clinical atlas representing its improvement or deterioration in relation with the anatomical location of electrodes and from a population of implanted patients. To the best of our knowledge, we reported for the first time a discrepancy between a very good motor improvement by targeting the postero-superior region of the STN and an inevitable deterioration of the categorical and phonemic fluency in the same region. Such atlases and associated analysis may help better understanding of functional mapping in deep structures and may help pre-operative decision-making process and especially targeting.

1. Introduction

1.1. Background

Parkinson's Disease (PD) is recognized as one of the most common neurological disorders, affecting 1% of people over the age of 60 years. It is the second most prevalent neurodegenerative disorder.

* Corresponding author at: MediCIS, INSERM, LTSI U1099, Faculté de Médecine CS 34317, F-35043 Rennes Cedex, France. Tel.: +33 633677214.
E-mail address: florent.lalys@univ-rennes1.fr (F. Lalys).

0165-0270/$ – see front matter © 2012 Published by Elsevier B.V.
http://dx.doi.org/10.1016/j.jneumeth.2012.11.002

One of the characters of PD is the apoptosis of the dopamine-rich neurons of the substantia nigra. Major symptoms are indeed characterized by abnormalities of motor functions, several of which predominate, but all do not necessarily occur in all individuals. While these PD-related symptoms can be treated with medical therapy, when it remains ineffective for some patients, a Deep Brain Stimulation (DBS) surgery (Benabid et al., 2000a,b; Krack et al., 2003) might be necessary according to strict patient inclusion criteria. This iterative procedure, initially approved by the Federal Drug Agency in U.S. in 1997 for essential tremor disorders, and in 2002 for PD, has gained much interest over the past decade and is now widely used by a large number of neurosurgical departments. The DBS anatomical target is based on the relief of symptoms and results of previous implantations only. The three major targets chosen by neurosurgeons according to the patients' symptoms are the Caudal part of the Ventro-Lateral thalamic nucleus (VLc), the medial Global Pallidus (GPm) and the Sub-Thalamic Nucleus (STN). Among these three deep brain structures, the STN became the most common target of high-frequency DBS in patients with severe motor disabled symptoms and no cognitive impairment (Benabid et al., 2000a,b; Lang and Lozano, 1998; Hamani et al., 2003; Bardinet et al., 2009; Volkmann et al., 2009).

1.2. Surgical procedure

During routine DBS surgery, two stages are mainly involved: pre-operative planning and the surgery itself. Pre-operative planning is the process of loading pre-operative patient's medical images (such as Computed Tomography and/or Magnetic Resonance Images), registering them together and proposing a 2D and/or 3D visualization interface to define the target localization in the Anterior and Posterior Commissures (AC–PC) plan. Mainly due to contrast and spatial resolutions limitations, the usual DBS targets are not easily visible on the MR images available to the surgeon, even though MRI offers better contrast than other medical imaging techniques (Dormont et al., 2010). Neurosurgeons directly localize the optimal target position on the T2 MR image and choose the trajectory of the electrode on patient's anatomical information. During this step, the additional help of an atlas may be necessary. In practice, experts manually localize AC–PC coordinates, midsagittal points and entry on the MR images of the patient. Finally, coordinates are automatically put in AC–PC space, then computed in a stereotactic coordinates system.

The surgical procedure is then performed under local anaesthesia. The trajectory estimated during planning is implemented with stereotactic frame based or frameless systems and used as an initial position that has to be refined. A few causes of discrepancy between chosen target and the final implant might appear, such as brain shift (Khan et al., 2008; Pallavaram et al., 2009), or patient's anatomical variability. An X-ray control is thus performed intra-operatively to confirm the initial placement and evaluate potential biases. Electrophysiological explorations are also performed to help neurosurgeons refine the placement of active electrode contacts. Similarly, neurologists may test the clinical effects with different settings for each contact to reach optimum placement. Changing frequency, voltage, stimulated contact and electrode trajectory, they reach optimum placement. Lastly, the surgeon anchors the electrode to the skull.

Even though STN DBS has demonstrated its efficiency for motor symptom improvement, questions remain concerning contact location providing the greatest motor improvement while producing the minimal neuropsychological and psychiatric side effects. Indeed, despite satisfactory motor improvements, several studies have reported adverse-events after DBS surgery affecting cognitive functions, emotion or behaviour (Parsons et al., 2006; Temel et al., 2006; Biseul et al., 2005; Dujardin et al., 2004; Houeto et al., 2002). In particular, Brücke et al. (2007), Kühn et al. (2005), Greenhouse et al. (2011), Lhommée et al. (2012) or Mallet et al. (2007) elucidated the role of STN in emotional processing, showing that STN DBS leads to behavioural complications. Similarly, Burrows et al. (2011) were interested in complications of STN DBS around the zona incerta, and York et al. (2009) looked at neuropsychological complications according to electrode location and trajectory. All these results suggest that the STN forms part of a broadly distributed neural network encompassing the associative and limbic circuits. Similarly, Witt et al. (2008) studied neuropsychiatric consequences of STN DBS. Based on this hypothesis, new works have then emerged. For instance, Karachi et al. (2005), or more recently Lambert et al. (2012) supported the hypothesis that the nucleus was separated in three regions: the limbic, associative and motor regions. Similarly, Lenglet et al. (2012) studied the basal ganglia and thalamic connections using high-resolution MR images. As outlined above, one of the major challenges in DBS is the identification of the target, which requires additional information and knowledge for indirect identification of such small structures during the pre-operative stage with the support of digital atlases.

1.3. Atlases

Brain atlases and atlas-based segmentation techniques have been developed to facilitate the accurate targeting of deep brain structures in patients with movement disorders (Schaltenbrand and Wahren, 1977; Talairach and Tournoux, 1988; Chakravarty et al., 2006; Yelnik et al., 2007; Bardinet et al., 2009; Lalys et al., 2009). Some digitized atlases aim at providing information with optimum spatial and intensity resolution, to allow better identification of structures, which is impossible with usual medical imaging techniques only. Histological atlases were thus created (Yelnik et al., 2007; Chakravarty et al., 2006) along with high-resolution MR based atlases (Aubert-Broche et al., 2006; Lalys et al., 2011). Both types of atlas have been successfully introduced in the targeting stage of standard DBS procedures.

The concept of probabilistic functional atlases, built from a population of previous surgical cases, was initially introduced by Nowinski et al. (2003, 2005, 2007). After a step of normalization within a common space, effective contacts are linked to preoperative electrophysiological recordings and clinical scores acquired during the stages of the procedure. Statistical techniques are used to study anatomical or functional variability between patients. Response to stimulation, electro-physiological recordings and clinical scores related to motor or cognitive evolution are all potential data that can be integrated into such atlases. This fusion of clinical and anatomical information allows an understanding of functional organization within deep-brain structures that helps in the identification of the optimal therapy zone for further patients. Finnis et al. (2003) and Guo et al. (2006) proposed probabilistic functional atlases by integrating intra-operative recordings. D'Haese et al. (2005, 2006) and Pallavaram et al. (2008, 2009) proposed a system to automatically predict the optimum target position according to atlases built from retrospective studies. More recently, D'Haese et al. (2010) proposed a fully integrated computer-assisted system called CRAnialVault. The system addresses the issue of data administration between the different stages of the therapy. It permits the centralization of various types of data acquired during the procedure and provides data visualization through data processing tools. A preliminary validation process in a clinical context, from planning to programming, is described and shows that the system provides genuine assistance to the surgical team.

Evaluation of DBS electrode implantation involves significant neurological and psychological follow-up estimated by clinical tests. Resulting clinical scores allow post-operative evaluation of the decrease in motor disorders and possible clinical side effects.

Please cite this article in press as: Lalys F, et al. Anatomo-clinical atlases correlate clinical data and electrode contact coordinates: Application to subthalamic deep brain stimulation. J Neurosci Methods (2012), http://dx.doi.org/10.1016/j.jneumeth.2012.11.002

Quantitative analysis of these data relative to the actual stimulated anatomical area would provide a better understanding of the DBS phenomenon, optimization of targeting and consequently better patient outcome.

As far as we know, no atlases have yet been proposed for representing the relationships between the STN anatomy and a broad panel of pre- and post-operative clinical scores. While most of these atlases use a single motor score for modelling the global outcome of the patient (e.g. Guo et al., 2006), we proposed in this paper to extend this research by adding pre- and post-operative motor, cognitive and neuropsychological scores of patients with Parkinson's disease and inclusion criteria for subthalamic stimulation. We thus introduce the concept of anatomo-clinical atlases and describe the methods for their computation. A high-resolution mono-subject template, already validated in the context of DBS (Lalys et al., 2011), along with a multi-subject template (Haegelen et al., in press), were tested as common spaces. Three motor and five neuro-psychological scores were then used to create anatomo-clinical atlases. The correlation was carried out using a dedicated non-supervised classification system and enabled the extraction of representative clusters to determine the optimum site for therapeutic STN DBS.

2. Materials and methods

The purpose of this study was to correlate and represent the anatomical position of electrode contacts with clinical outcomes in STN DBS. Firstly, a method for automatic extraction of electrode contacts for each patient was developed. Secondly, an accurate patient images-to-template registration step was studied. Thirdly, the integration of clinical scores from a clinical database was used to extract representative anatomo-clinical clusters, through non-supervised classification.

2.1. Data

The study population consisted of 30 patients (14 women and 16 men, mean age: 60 ± 5 years) with idiopathic PD who had bilateral STN DBS according to selected inclusion (Langston et al., 1992; Lang and Lozano, 1998; Krack et al., 1998). In particular, one of the inclusion criteria is the improvement of 50% in UPDRS III score during the pre-operative levodopa challenge test. All patients had one pre-operative 3-T T1-weighted MR (Size: $256 \times 256 \times 182$, resolution: $1\,mm \times 1\,mm \times 1\,mm$, Philips Medical Systems) and two CT scans (Size: $203 \times 203 \times 155$, resolution: $0.44\,mm \times 0.44\,mm \times 0.6\,mm$, in post-operative acquisition and $0.5\,mm \times 0.5\,mm \times 0.6\,mm$ in pre-operative acquisition, GE Healthcare VCT 64). Pre-operative scans were acquired after attachment to the patient's head of a stereotactic Leksell frame, under local anaesthesia. All images were de-noised using the Non-local means algorithm (Coupe et al., 2008) and a bias correction algorithm based on intensity values (Mangin, 2000) was also applied to MR images. This study was part of a larger clinical study approved by the local ethical review board.

To assess the global patient outcome, we first chose three motor scores: the UPDRS III (Unified Parkinson's Disease Rating Scale, part III) score (Fahn and Elton, 1987), the Schwab & England scale, and the Hoehn & Yahr scale. For each score, patients were tested without medication (Dopa OFF) immediately prior to surgery (DBS OFF) and three months after it under stimulation (DBS ON), also without medication. We then selected five neuropsychological scores:

- The categorical and the phonemic verbal fluency tests (Troyer et al., 1998) that determine the ease with which patients can produce words.
- The Stroop test (Stroop, 1935) that computes the mental vitality and flexibility.
- The Trail Making Test (Reitan, 1958) that determines visual attention and task switching.
- The Wisconsin Card Sorting Test (Psychological assessment and resources, 2003) that estimates the ability to display flexibility in the face of changing schedules of reinforcement.
- The MATTIS score (Mattis, 1988) that tests global cognitive efficiency.

2.2. Contact localization

For each electrode, the spatial coordinates of the contacts were automatically computed from post-operative CT images by modelling the electrode's axis. We developed a new segmentation technique based on the hypo-signal artefacts (white artefacts) created on CT scans and corresponding to the electrodes. Every CT scan was first simply linearly registered to a reference patient CT. On this reference image, a mask was defined including the two electrodes and entirely excluding the skull. An intensity threshold was applied in order to extract every hypo-signal voxel of both electrodes per patient. Along with a connected component approach for retrieving noise, for each slice, the barycentre of extracted voxels was computed to model the electrodes' axis. By keeping 10 mm from the tip of the electrode, we then performed regression in order to model the area where contacts can finally be obtained by applying geometry constraints of electrode 3389 from Medtronic Neuro-Modulation, USA (Fig. 1.). This automatic procedure was performed for post-operative CT of each patient and gave us all contact locations. It was validated in Mehri et al. (2012) and gave us an error of 0.96 ± 0.33 mm using a linear regression for the modelling of the electrode's axis.

2.3. Patient to template registration workflow

Patient contacts were warped into a MR template as a common anatomical space for allowing retrospective population statistical analysis. We compared the impact of mono-subject vs. multi-subject MR high-resolution templates on the patient/template non-linear registration accuracy. In opposition to pure histological templates, MR templates are correctly representing the in vivo anatomy of the brain. We also compared two non-linear registration methods.

The mono-subject template was created from 15 3T MR acquisitions of a healthy 45 year-old male, which were processed and averaged. This high-resolution 3T MRI template (namely the Jannin15), was constructed and assessed by Lalys et al. (2011). The multi-spectral multi-subject, unbiased non-linear average, PD template was made from 57 T1w images of patients with PD (namely the Avg57), thus providing a high-resolution/high signal-to-noise ratio template (Haegelen et al., in press). This template allows the specific developmentally important age-ranges and atrophy of PD patients to be taken into account.

The registration workflow was composed of a linear CT to MR patient images registration, a global affine MR-to-template registration, a local affine MR-to-template registration with a mask on deep structures, and a final non-linear registration. Using this procedure the contact positions could be precisely warped into a reference space. We compared the accuracy of two non-linear registration algorithms: the demons approach (www.itk.org) that was used in our previous studies, and the Advanced Normalization ToolS (ANTS) non-linear deformation algorithm used in Symmetric Normalization (SyN) mode that has been shown to be highly effective in the context of MR brain imaging registration (Klein et al., 2009).

For both validation studies, we followed a landmark-based validation approach. Ten anatomical structures were identified within

Please cite this article in press as: Lalys F, et al. Anatomo-clinical atlases correlate clinical data and electrode contact coordinates: Application to subthalamic deep brain stimulation. J Neurosci Methods (2012), http://dx.doi.org/10.1016/j.jneumeth.2012.11.002

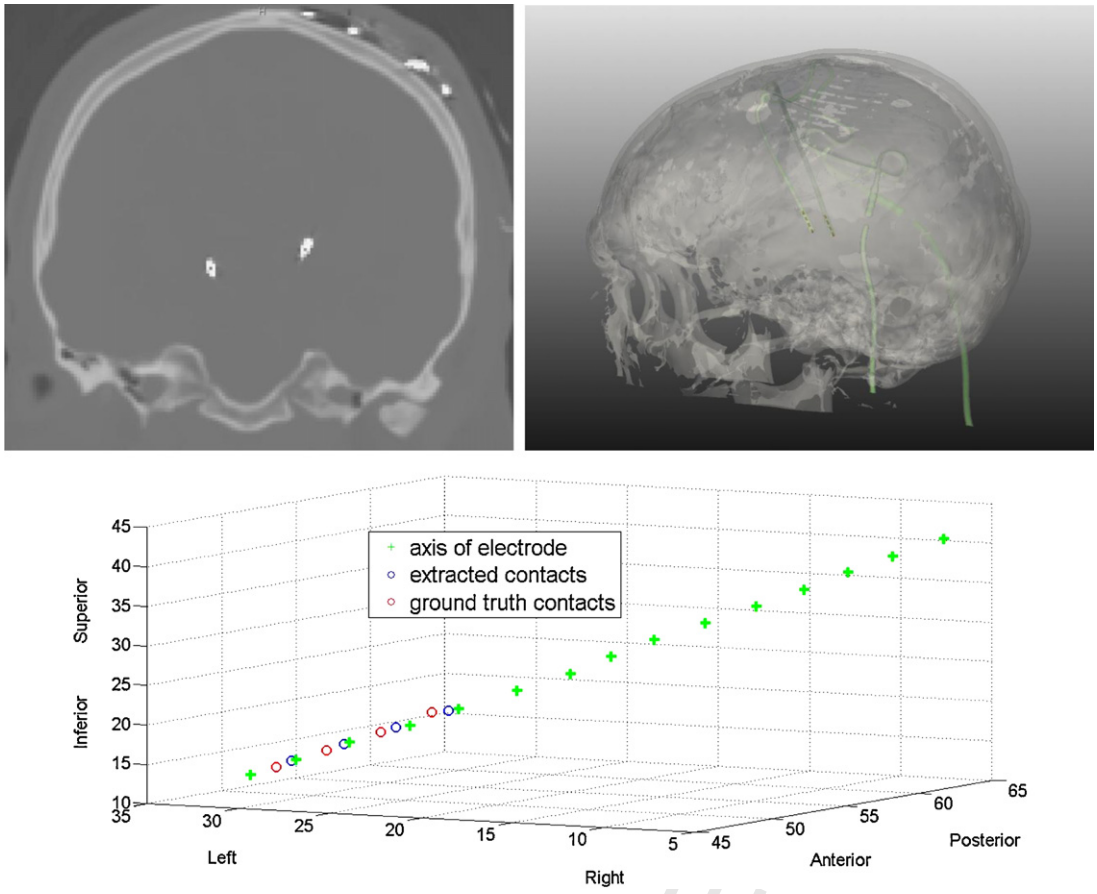

Fig. 1. Upper left: post-operative CT scan of one patient with PD and bilateral STN-DBS. Upper right: segmentation of the patient's skull, the 2 electrodes and the 8 electrode contacts. Below: electrode's axis, the 4 extracted contacts and the 4 ground truth contacts for the left side.

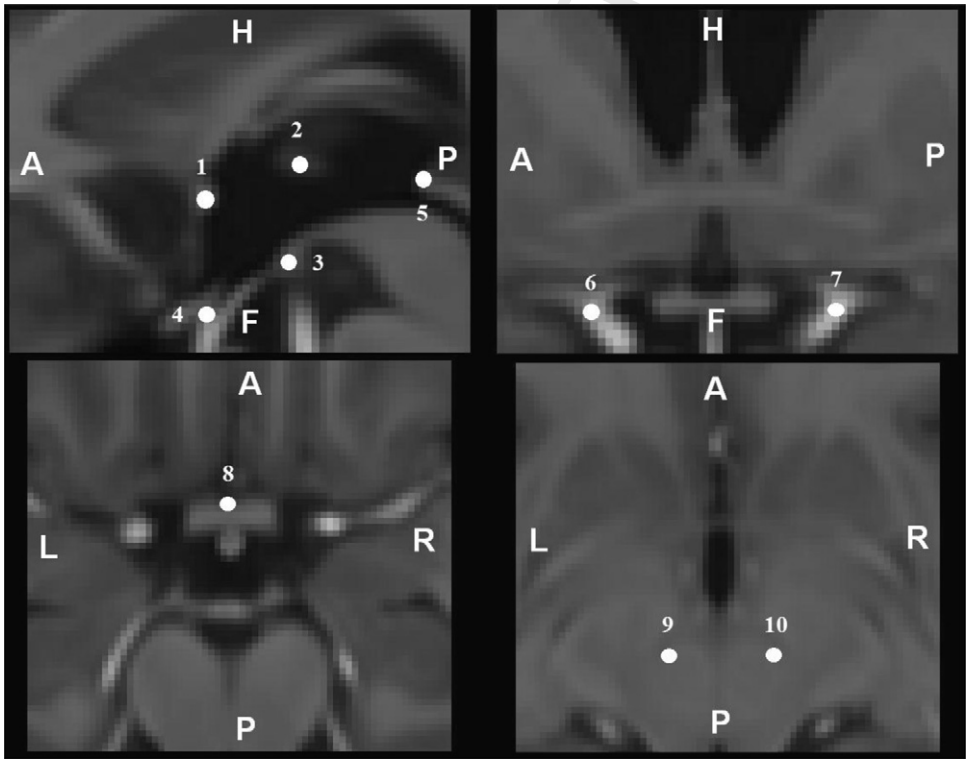

Fig. 2. Anatomical landmarks used for the validation study. 1: Anterior Commissure. 2: Interthalamic adhesion on the middle of the axial slice. 3: Posterior Commissure. 4: Infundibular recesse. 5: Middle of the mamillar bodies. 6,7: Left and right internal carotid division into anterior and middle cerebral arteries. 8: Centre of the anterior portion of the optic chiasma. 9,10: Centres of the left and right red nuclei.

Please cite this article in press as: Lalys F, et al. Anatomo-clinical atlases correlate clinical data and electrode contact coordinates: Application to subthalamic deep brain stimulation. J Neurosci Methods (2012), http://dx.doi.org/10.1016/j.jneumeth.2012.11.002

deep-brain structures (Fig. 2) and manually identified in the images by an expert. Placement of these landmarks on the one hand on the template, and on the other hand on 15 wrapped MR images, allowed us to compute a global registration error. Considering that the intra-subject registration between the CT scan and the MR image was accurate, we only validated the MR-to-template registration. We first compared both templates by keeping the classical linear registration process along with the non-linear Demons algorithm. We then compared, using the best template found, both non-linear registrations (i.e. Demons Vs ANTS-SyN) using a Student's *t*-test.

2.4. Anatomo-clinical atlases

For all scores and for representing the degree of improvement or worsening of the patient, the difference between DBS ON and DBS OFF values was computed. In order to represent all improvement or worsening of patients on a similar scale, all clinical scores were statistically normalized. On each score, we subtracted the mean and divided by the variance of the dedicated score. After normalization, the data closely followed a normal distribution (with mean = 0 and standard deviation = 1) and were more easily usable for data variation comparisons.

For each score, an atlas was computed as the list of active contact coordinates from all patients associated with the corresponding difference value. The active contacts were those at three months post-surgery. 3D visualization consisted in displaying the list of points represented with a colour code related to the patient clinical scores. Each clinical score can therefore create one anatomo-clinical atlas. Due to random errors or missing values in reporting scores, the initial clinical score dataset of 30 patients dropped to 23 for the motor analysis, but remained at 30 for the neuropsychological analysis.

2.5. Non-supervised classification

After atlas construction, we performed a segmentation step using non-supervised techniques. Hierarchical Ascendant Classification (HAC) was used on clinical scores merged with coordinates to search homogeneous groups of patients and extract general clinical trends. Feature vectors were composed of four features: the value of the *x*-axis, *y*-axis, *z*-axis and the score difference value. HAC operates by successively merging pairs of existing clusters, where the next pair of clusters to be merged is chosen as the pair with the smallest distance. This linkage between clusters *a* and *b* was performed using the Ward criterion along with the weighted Euclidean distance:

$$d^2(a,b) = n_a n_b \frac{\sum_{k=1}^{M} w_k |\overline{x_{ak}} - \overline{x_{bk}}|}{n_a + n_b}$$

where $\overline{x_a} = 1/n_a \sum_{i=1}^{n_a} x_{ai}$ is the centroid of cluster *a* (resp. *b*), n_a (resp. n_b) is the number of objects in cluster *a* (resp. *b*), and w_k are the weights, specified by $w_1 = w_2 = w_3 = 1/12$ and $w_4 = 3/4$. The dendrogram was cut in order to obtain two or three clusters for each clinical score. Validation of the non-supervised classification was performed with an ANOVA test.

3. Results

The registration error was computed for the different combinations of non-linear registrations and templates. First, results of Table 1 show that the new multi-subject template was significantly better than the mono-subject one (*p*-value = 0.025).

Table 2 then shows that the new non-linear registration method (ANTS-SyN) gave best results compared to the Demons algorithm (*p*-value = 0.05). For the rest of the study, the two new parameters were then conserved, providing a global registration error of 0.98 ± 0.17 mm. Patient's contacts were also warped in the Talairach space for clinical verification. The origin of the electrode contact coordinates was the midpoint between the AC and the PC points. Three months after surgery, the mean position of the active electrode's contacts for the left electrodes was $X = +14.33$ mm for the lateral direction, $Y = -1.79$ mm for antero-posterior direction, $Z = -1.01$ mm for the dorso-caudal direction, and $X = -14.65$ mm, $Y = -1.88$ mm, $Z = -0.77$ mm for the right electrodes. The stimulation parameters used were frequency at 130 Hz, pulse duration for 60 microseconds for all the patients and a mean voltage of 2.14 ± 0.34 V.

For all following figures, we represent the results in the Talairach space as well as in Avg57 template to improve clinical representation and interpretation. For each clinical score, clustering was performed for both hemispheres independently. For each clinical score, we noticed that the group of patients (clusters) that were extracted for both hemispheres were identical. The *x*-axis represents the left-right direction, the *y*-axis represents the antero-posterior direction, and the *z*-axis represents the caudo-cranial direction. The scale of figures is shown in mm. Fig. 3 shows a greater improvement of UPDRS III for cluster Blue compared to clusters Red and Green ($p = 10^{-6}$). Majority of the contacts of the cluster Blue were in the postero-superior region of the STN. Hoehn & Yahr and Schwab & England scores showed similar results, but with a fuzzy definition of clusters ($p = 5.10^{-2}$).

Fig. 4 shows a deterioration of the categorical fluency in the posterior region (cluster Red), and an improvement in the antero region (cluster Blue) ($p = 10^{-4}$). For the phonemic fluency we found a general deterioration for all patients, without apparent separation of clusters. STROOP score analysis (Fig. 5) indicated score improvement in the postero-superior region (cluster Red), and deterioration in the antero-inferior region ($p = 10^{-5}$) (cluster Blue). For the three other neuropsychological scores (Trail Making Test, Wisconsin Card Sorting Test, MATTIS score), no significant clusters were found ($p > 5.10^{-2}$). Table 3 summarizes results of the analysis using the different clinical scores.

4. Discussion

This article reports about the construction of anatomo-clinical atlases in patients with STN stimulation and severe disabled Parkinson's disease. To the best of our knowledge, we reported for the first time a discrepancy between a very good motor improvement by targeting the postero-superior region of the STN and an inevitable deterioration of the categorical and phonemic fluency in the same region. These results were provided by the use of tools already validated but never used together to provide the association of clinical scores with electrode contacts within a normalized space in the context of STN DBS.

4.1. Contact localization and representation

Many publications advocate the use of post-operative MRI to determine the electrode's contact coordinates (Saint-Cyr et al., 2002; Pollo et al., 2007) despite the possible adverse effects related to MRI acquisition with implanted DBS electrodes (Medtronic, 2006). The use of MRI has recently been validated by Lee et al. (2010) with a study showing that there were no significant discrepancies between the centres of electrodes estimated by CT and MRI. In this project, the spatial coordinates of the 4 contacts per electrode were automatically computed from post-operative CT images. The automatic contact localization algorithm gave us satisfactory results with an average error of 0.96 ± 0.33 mm (Mehri et al., 2012). This error, even quite low, has to be taken into account in the final

Please cite this article in press as: Lalys F, et al. Anatomo-clinical atlases correlate clinical data and electrode contact coordinates: Application to subthalamic deep brain stimulation. J Neurosci Methods (2012), http://dx.doi.org/10.1016/j.jneumeth.2012.11.002

Table 1
Landmark-based validation for the comparison of the Jannin15 vs. Avg57 templates on patient to atlas non-linear registration using Demon's method.

	Mean registration error (mm)	Std deviation (mm)	Test student
Jannin15 template + Demons non-linear registration	1.23	0.12	p-value = 0.025
Avg57 template + Demons non-linear registration	1.15	0.09	

Table 2
Landmark-based validation for the comparison of the Demons vs. ANTS-SyN non-linear registration methods.

	Mean registration error (mm)	Std deviation (mm)	Test student
Avg57 template + Demons non-linear registration	1.15	0.09	p-value = 0.05
Avg57 template + ANTS-SyN non-linear registration	0.98	0.17	

cluster analysis. Considering the relative small size of the STN and its sub-regions, this bias will still have to be minimized using more robust automatic segmentation algorithms.

Comparison of electrode positions of STN DBS estimated in the immediate post-operative CT with those estimated 6 months after surgery showed that they may contain some discrepancies (Kim et al., 2010). Results also indicated that it is often due to the extensive pneumocephalus. Ideally, this bias could be reduced by comparing clinical scores evaluated 6 months after the surgery with a post-operative CT acquired within the same period.

We modelled the signal by a point corresponding to the centre of the artefact. For further developments, it will be crucial to integrate the influence of stimulation on the surrounding biological tissues. Some studies on the modelling of tissues and electrical influence of electrodes in the context of DBS have recently been published (Buston et al., 2011). Complete DBS modelling would integrate all of these data to provide the highest possible precision.

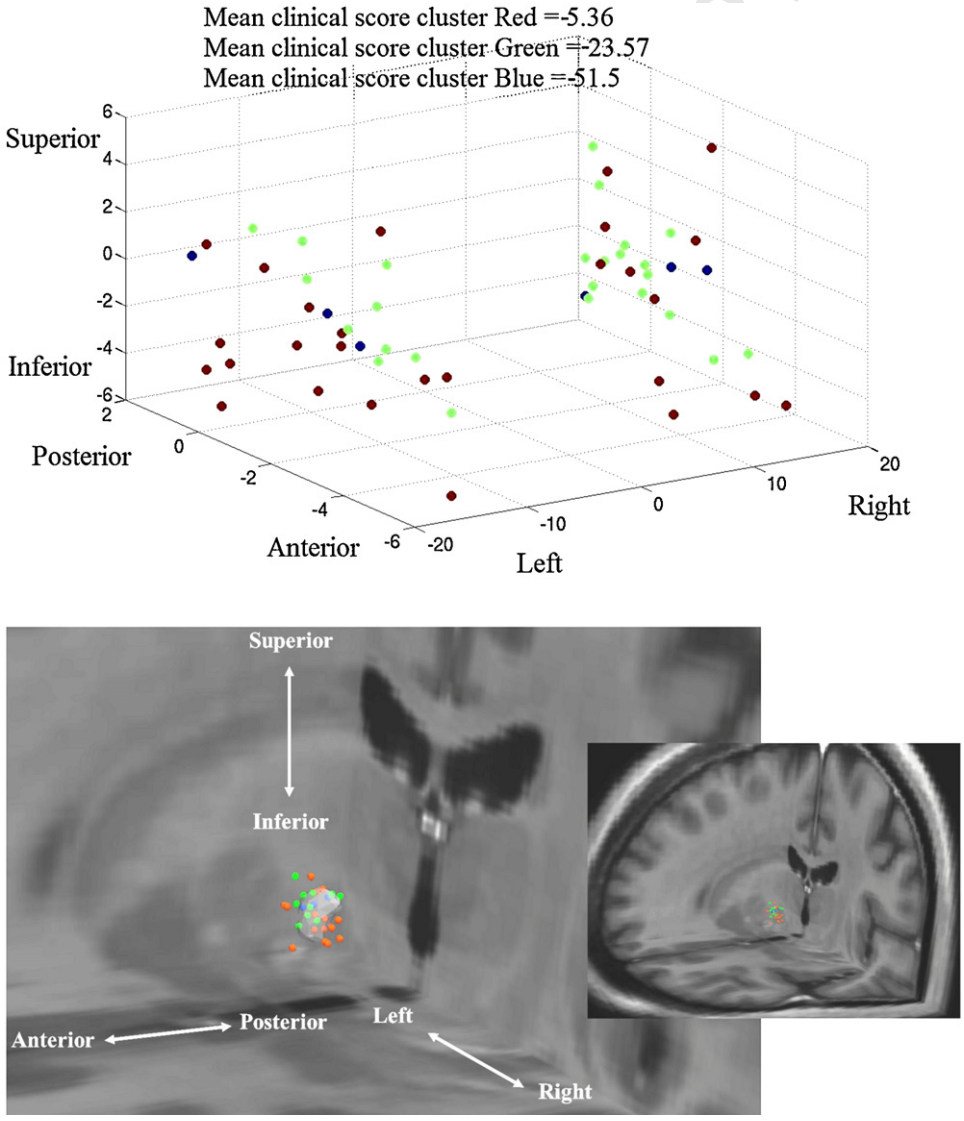

Fig. 3. UPDRS III analysis, with the cluster display in Talairach coordinates (above), and the cluster display in the template space for the left hemisphere with the STN (below).

Please cite this article in press as: Lalys F, et al. Anatomo-clinical atlases correlate clinical data and electrode contact coordinates: Application to subthalamic deep brain stimulation. J Neurosci Methods (2012), http://dx.doi.org/10.1016/j.jneumeth.2012.11.002

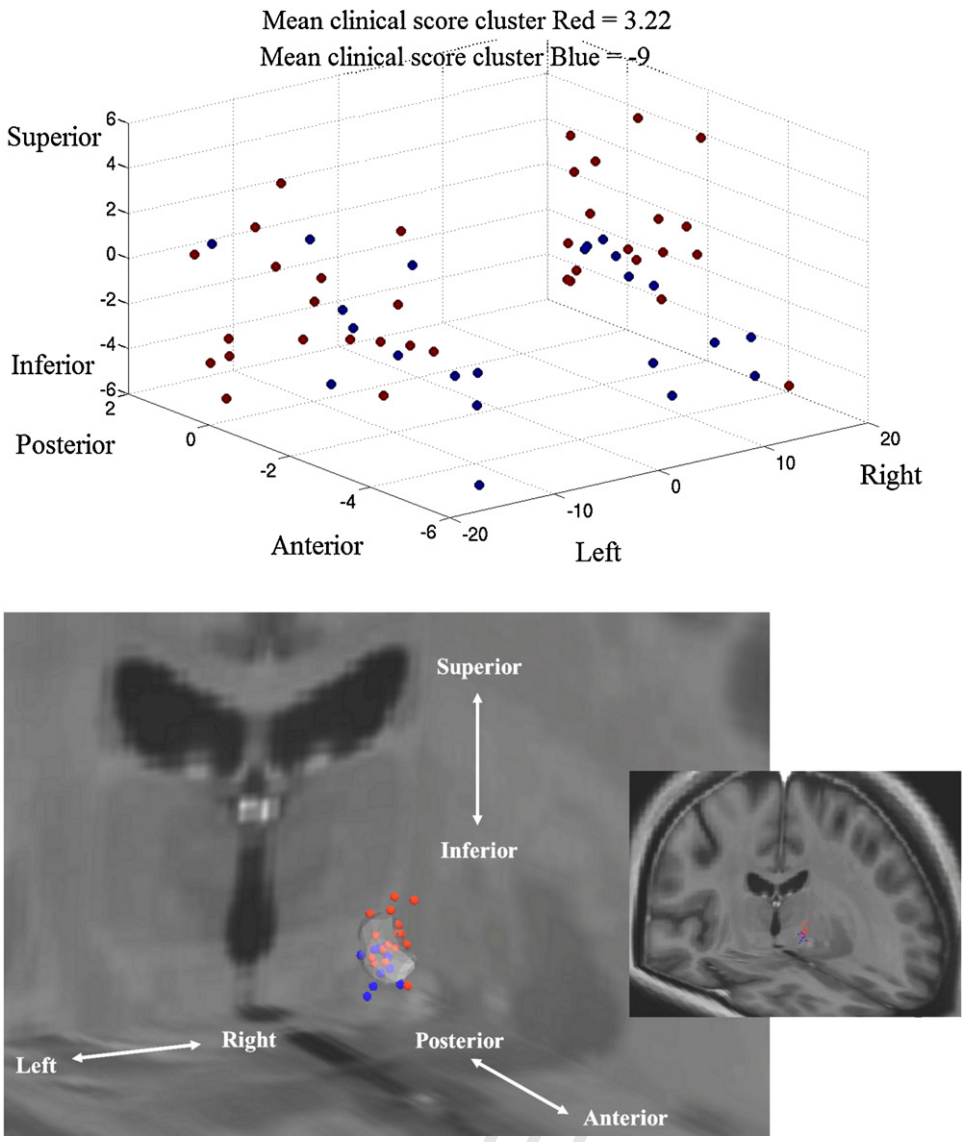

Fig. 4. Categorical fluency analysis, with the cluster display in Talairach coordinates (above), and the cluster display in the template space for the right hemisphere with the STN (below).

4.2. Template and registration workflow

We compared the impact of mono-subject vs. multi-subject MR high-resolution templates on the patient/atlas non-linear registration accuracy. Both templates allowed the production of reference images with a high degree of anatomical detail, both for deep-brain structures and for the cerebral cortex. The accuracy of the patient images-to-template registration is an important step, which may considerably impact the quality of the findings. In DBS, major sources of errors are due to the identification of basal ganglia from patient-specific images. Therefore, during the procedure, we added a local registration involving targeted structure (STN), intended to improve basal ganglia registration. Results of the template-to-patient registration comparison have shown that

Table 3
Summarization of clusters found for each clinical score, i.e. the number of patients per cluster, the dedicated mean clinical score, the clinical signification of the mean clinical score and the major STN zone of stimulation of the patients belonging to this cluster.

Clinical scores	Cluster	Number of patients	Mean clinical score (Post-pre-op)	Clinical signification	Major STN zone of stimulation
UPDRS III	*Cluster Blue*	3	−51.5	Very good improvement	Postero-superior region
	Cluster Green	11	−23.6	Good improvement	Superior and Posterior regions
	Cluster Red	15	−5.4	Stabilization	Anterior and inferior regions
Categorical fluency	*Cluster Blue*	11	−9	Improvement	Antero region
	Cluster Red	18	3.2	Deterioration	Posterior region
STROOP	*Cluster Blue*	13	−5	Deterioration	Antero-inferior region
	Cluster Red	15	2.6	Improvement	Postero-superior region
Others	*No significant clusters found*				

Please cite this article in press as: Lalys F, et al. Anatomo-clinical atlases correlate clinical data and electrode contact coordinates: Application to subthalamic deep brain stimulation. J Neurosci Methods (2012), http://dx.doi.org/10.1016/j.jneumeth.2012.11.002

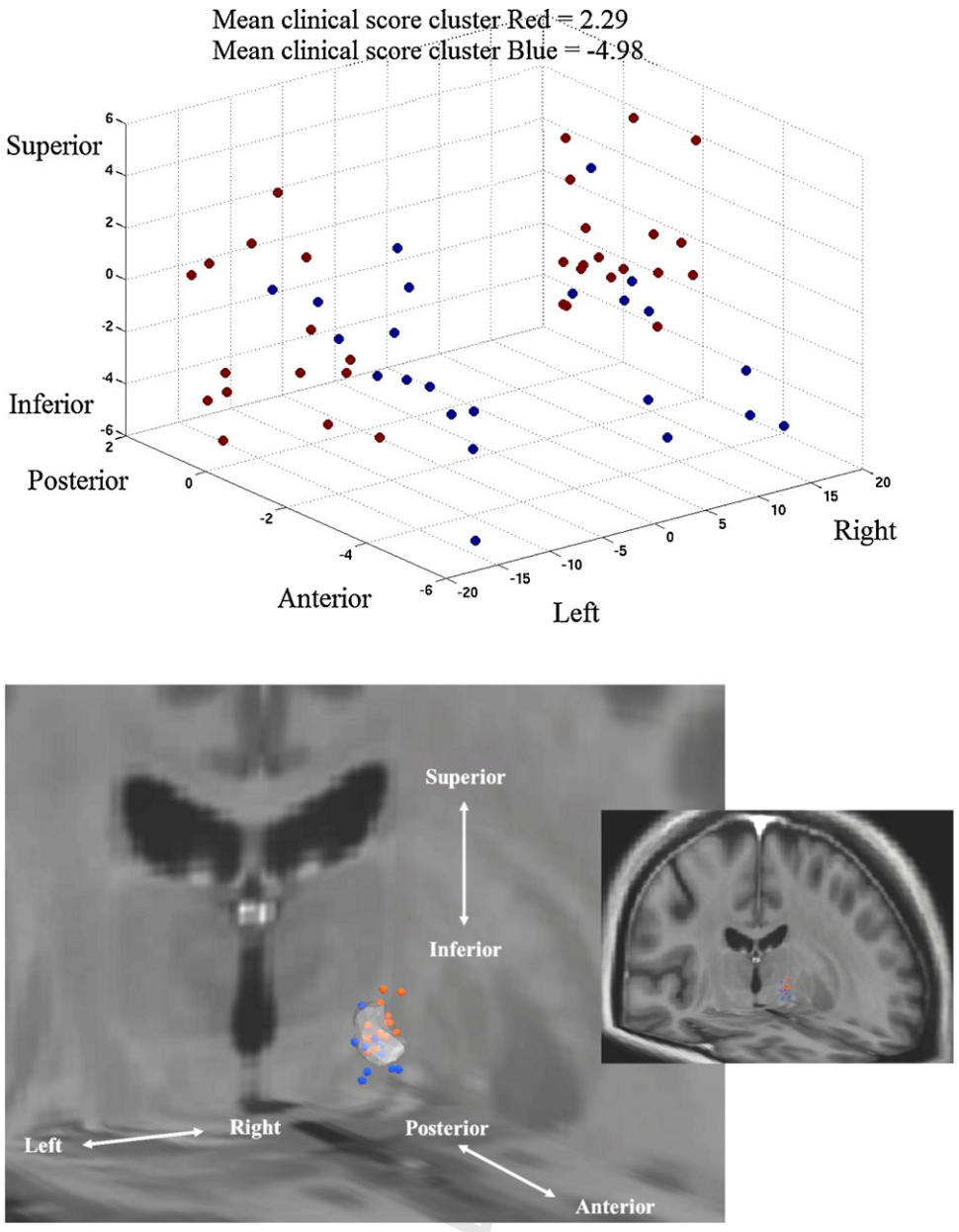

Fig. 5. STROOP analysis, with the cluster display in Talairach coordinates (above), and the cluster display in the template space for the right hemisphere with the STN (below).

the new multi-subject template increases the accuracy of a patient-to-template basal ganglia registration. This is explained by the fact that the single subject template did not take into account brain atrophy of the patient population. The impact of this new template was significant and it has improved not only registration quality (0.98 mm) but also retrospective visualization. During the registration workflow, intra-subject rigid registration appears to be very effective, especially when native acquisitions are subject to a step of reliable pre-processing as we performed in our registration procedure. On the contrary, the patient-to-template registration procedure, including linear and non-linear registrations steps, was subject to small errors that can explained this registration error of 0.98 mm. Similarly to the localization of the electrode contacts, this bias has to be taken into account when analysing the final cluster results.

Many active contacts are located outside the STN within atlases. This can be partially explained by the error induced during the warping step, though other explanations could be put forward. First, the electrical stimulation zone is in fact larger than the simple contact position, recovering a region wide enough to accept a targeting uncertainty. It is known, in any case, that the field of stimulation can have a spread of up to 2 mm within the brain (Buston et al., 2011). Secondly, deep-brain tissues and nerves are deeply interconnected and nerves at the periphery of structures have an influence on the structure itself.

The coordinates of the stimulated contacts were more lateral than those previously reported (Krack et al., 2003; Dujardin et al., 2004; Houeto et al., 2002). One explanation could be that the targeting in our study was based on 3T MRI and not on ventriculography as in other centres. The visualization of the STN on T2 pre-operative MRI allowed direct targeting instead of probabilistic targeting based on the Talairach atlas. The neurosurgeons attempted to place the electrode in the postero-superior part of the STN as they knew that it is involved in motor component of the STN (Rodriguez-Oroz et al., 2001; Theodosopoulos et al., 2003).

Please cite this article in press as: Lalys F, et al. Anatomo-clinical atlases correlate clinical data and electrode contact coordinates: Application to subthalamic deep brain stimulation. J Neurosci Methods (2012), http://dx.doi.org/10.1016/j.jneumeth.2012.11.002

4.3. Clinical scores

Each clinical score was used to extract representative clusters. Compared to clustering on clinical scores only, adding coordinates allows a better definition of clusters and a better understanding of DBS efficiency according to contact locations. Motor and neuropsychological scores were analysed to assess the patient outcome (Benabid et al., 2000a,b; Brontë-Stewart et al., 2010). Other teams have also focused on the analysis of clinical scores in the context of STN DBS (Guehl et al., 2007; Lanotte et al., 2002).

In our procedure, the main issue was the inability to separate the response to DBS stimulation of the right and left contacts. Each test was performed with both activated contacts. Separate evaluations would involve many hours without medication and stimulation in order to lose previous therapeutic and stimulation effects. In the pre-operative targeting procedure, surgeons first localized the optimum target position of one side, and the target position of the other side was automatically computed from the definition of the mid-sagittal line. These targets were used as an initial position that had to be refined per-operatively.

Other variables that could have been taken into account are the different contact parameters, i.e. the frequency, pulse duration and voltage. From the 30 patients in our study, these parameters did not differ among patients, so we did not include the stimulation parameters in the study. Moreover, the standard deviation of the stimulation voltage was low and not sufficiently discriminant to be included.

Because of their low granularity, values of the Schwab & England and Hoehn & Yahr scales turned out to be less representative than UPDRS III. Moreover, our method was more useful for quantitative continuous data than for quantitative discontinuous data. For this reason, even though the results of motor scores studies were almost identical, the visualization of the atlas containing the UPDRS III provides more information. Using these clinical data, the postero-superior region has been found to be the most effective region for motor improvement. This follows conclusions of previously published work on the topic (Guehl et al., 2007; Lanotte et al., 2002), and can be explained by the fact that this part of the STN (usually named the dorso-lateral part) is involved in sensory and motor functions (Maks et al., 2009). Indeed, as shown in the introduction, a subdivision of the STN into a ventromedial associative and a medial limbic (psychology, mood) territories is described in the literature. Recent studies (Karachi et al., 2005; Lambert et al., 2012), stated that the motor region was situated in the posterior portion of the nucleus. Our results related to motor improvements therefore support this hypothesis. Moreover, this subdivision can explain that the antero-inferior (corresponding to the limbic territory) region has shown significant neuropsychological side effects such as the deterioration of the Stroop score. In Lambert et al. (2012), the limbic zone was found to be in the anterior portion of the STN. Results on the Stroop score are also quite satisfactory as it can be explained by recent discoveries on STN territories. Lastly, our study highlighted at our knowledge for the first time, that the categorical fluency was improved in the anterior region of the STN, whereas the categorical fluency was worse in its postero-superior region. Moreover, the phonemic fluency was worse after STN stimulation whatever the region of the STN stimulated. This last result was not surprising as the deterioration of phonemic verbal fluency is one of the most observed side effects in STN DBS, though the phenomenon is not really understood (Temel et al., 2006; Saint-Cyr et al., 2000). The deterioration of the phonemic fluency seems to be impossible to avoid after STN stimulation and the categorical fluency only improved in the anterior region that is not the best region in terms of motor improvement. We can imagine multiple sub-regions within the STN where the stimulation may involve these side effects, but the extraction of finer spatial clusters would require a larger study population. Our results could also demonstrate that the STN is not so well subdivided into three different functional territories but the motor, associative and limbic territories are more probably mixed due to diffused interneuron's connection.

Lastly, concerning all other neuropsychological scores (Trail Making Test, Wisconsin Card Sorting Test, MATTIS score), no clusters were clearly defined, resulting in small statistical differences. With our current data, no statistical clusters could be extracted from these scores yet, either because of the number of patients associated with the different bias of the analysis, or because no significant effects were observed amongst patients for these specific clinical scores.

5. Conclusion

In this paper, we focused on identifying optimum sites for STN DBS by studying symptomatic motor improvement along with neuropsychological side effects. The underlying mechanisms of action of DBS surgery have not yet been identified. The concept of anatomo-clinical atlases, introduced in this paper, allows the integration, within a single coordinate system, of a digitized brain MRI template, previous target coordinates of implantations, and various clinical scores. Each clinical score produced one anatomo-clinical atlas, associating the degree of improvement or worsening of the patient with its active contacts. Additionally, non-supervised classification was performed on scores and coordinates to extract clusters for determining optimum electrode contact coordinates. We showed how to extract knowledge gained from population data based on the correlation between anatomical location of contacts and clinical data. To the best of our knowledge, we reported for the first time a discrepancy between a very good motor improvement by targeting the postero-superior region of the STN and an inevitable deterioration of the categorical and phonemic fluency in the same region. The proposed anatomo-clinical atlases were created to provide the surgeons with additional assistance for better understanding of DBS-related phenomena. It could find its application in pre-operative planning (Dawant et al., 2007; Stancanello et al., 2008) as well as for post-operative assessment (Lalys et al., 2009). As targeting is mainly based on the surgeon's knowledge and experience, it could serve as an additional source of information obtained from retrospective studies for reducing time and predicting motor outcome and possible post-operative adverse-effects. The underlying challenge would be to reduce the intra-operative time required for electrode contact adjustment by microelectrode recordings. The actual local anaesthesia would be replaced by a general anaesthesia, which would completely alter the surgical routine by reducing surgical staff workload, improving patient care and increasing medical safety. Alternatively, such atlases also provide an understanding of previous interventions that did not give satisfactory results. In such cases, active contacts of a new patient can be warped into the common space, displayed for post-operative assessment, and inserted into a new analysis for updating the atlases. This work yields many flourishing studies in the field, including further clinical data such as quality of life or cognitive criteria. Q7

Uncited references Q8

Fonov et al. (2011), Huebl et al. (2011) and Zaidel et al. (2010).

Acknowledgments

The authors would like to acknowledge Alexandre Bonnet for his contribution to the registration validation studies, Dr Eduardo Pasqualini, Vladimir Fonov. The authors would like to thank the

Please cite this article in press as: Lalys F, et al. Anatomo-clinical atlases correlate clinical data and electrode contact coordinates: Application to subthalamic deep brain stimulation. J Neurosci Methods (2012), http://dx.doi.org/10.1016/j.jneumeth.2012.11.002

French Research Agency (ANR) for funding this study through the ACouStiC project.

References

Aubert-Broche B, Evans AC, Collins L. A new improved version of the realistic digital brain phantom. Neuroimage 2006;32:138–45.
Bardinet E, Bhatttacharjee M, Dormont D, Pidoux B, Malandain G, Schüpbach M, et al. A three-dimensional histological atlas of the human basal ganglia. II. Atlas deformation strategy and evaluation in deep brain stimulation for Parkinson disease. J Neurosurg 2009;110:208–19.
Benabid AL, Krack P, Benazzouz A, Limousin P, Koudsie A, Pollak P. Deep brain stimulation of the subthalamic nucleus for Parkinson's disease: methodologic aspects and clinical criteria. Neurology 2000a;55:40–4.
Benabid AL, Koudsié A, Benazzouz A, Fraix V, Ashraf A, Le Bas JF, et al. Subthalamic stimulation for Parkinson's disease. Arch Med Res 2000b;31:282–9.
Biseul I, Sauleau P, Haegelen C, Trebon P, Drapier D, Raoul S, et al. Fear recognition is impaired by subthalamic nucleus stimulation in Parkinson's disease. Neuropsychologia 2005;43:1054–9.
Burrows AM, Ravin PD, Novak P, Peters ML, Dessureau B, Swearer J, et al. Limbic and motor function comparison of deep brain stimulation of the zona incerta and subthalamic nucleus. Neurosurgery 2011;70(1):125–30.
Buston CR, Cooper SE, Henderson JM, Wolgamuth B, McIntyre CC. Probabilistic analysis of activation volumes generated during deep brain stimulation. Neuroimage 2011;54(3):2096–104.
Brontë-Stewart H, Louie S, Batya S, Henderson JM. Clinical motor outcome of bilateral subthalamic nucleus deep-brain stimulation for Parkinson's disease using image-guided frameless stereotaxy. Neurosurgery 2010;67(4):1088–93.
Brücke C, Kupsch A, Schneider GH, Hariz MI, Nuttin B, Kopp U, et al. The subthalamic region is activated during valence-related emotional processing in patients with Parkinson's disease. Eur J Neurosci 2007;26:767–74.
Chakravarty M, Bertrand G, Hodge CP, Sadikot AF, Collins DL. The creation of a brain atlas for image guided neurosurgery using serial histological data. Neuroimage 2006;30(2):359–76.
Coupe P, Yger P, Prima S, Hellier P, Kervrann C, Barillot C. An optimized blockwise non local means denoising filter for 3D magnetic resonance images. IEEE Trans Med Imaging 2008;24(4):425–41.
Dawant B, D'Haese PF, Pallavaram S, Li R, Yu H, Spooner J, et al. The VU-DBS project: integrated and computer-assisted planning, intra-operative placement, and post-operative programming of deep-brain stimulators. SPIE Med Imaging 2007;6509(1):650907.
D'Haese PF, Cetinkaya E, Konrad PE, Kao C, Dawant BM. Computer-aided placement of deep brain stimulators: from planning to intraoperative. IEEE Trans Med Imaging 2005;24(11):1469–78.
D'Haese PF, Pallavaran S, Yu H, Spooner J, Konrad PE, Dawant BM. Deformable physiological atlas-based programming of deep brain stimulators: a feasability study. Utrecht, The Netherlands: WBIR; 2006, p. 144–50.
D'Haese PF, Pallavaram S, Li R, Remple MS, Kao C, Neimat JS, et al. CranialVault and its CRAVE tools: a clinical computer assistance system for deep brain stimulation (DBS) therapy. Med Image Anal 2010;16(3):744–53.
Dormont D, Seidenwurm D, Galanaud D, Cornu P, Yelnik J, Bardinet E. Neuroimaging and deep brain stimulation. Am J Neuroradiol 2010;31(1):15–23.
Dujardin K, Blairy S, Defebvre L, Krystkowiak P, Hess U, Blond S, et al. Subthalamic nucleus stimulation induces deficits in decoding emotional facial expressions in Parkinson's disease. J Neurol Neurosurg Psychiatry 2004;75:202–8.
Fahn Y, Elton R. Unified Parkinson's disease rating scale. In: Fahn S, Marsden C, Calne D, Goldstein M, editors. Recent developments in Parkinson's disease, 2. Florham Park, NJ: Macmillan; 1987. p. 153–63.
Finnis KW, Starreveld YP, Parrent AG, Sadikot AF, Peters TM. Three-dimensional database of subcortical electrophysiology for image-guided stereotactic functional neurosurgery. IEEE Trans Med Imaging 2003;22(1):93–104.
Fonov V, Evans AC, Botteron K, Almli CR, McKinstry RC, Collins DL. Unbiased average age-appropriate atlases for pediatric studies. Neuroimage 2011;54:313–27.
Greenhouse I, Gould S, Houser M, Hicks G, Gross J, Aron AR. Stimulation at dorsal and ventral electrode contacts targeted at the subthalamic nucleus has different effects on motor and emotion functions in Parkinson's disease. Neuropsychologia 2011;49:528–34.
Guehl D, Edwards R, Cuny E, Burbaud P, Rougier A, Modolo J, et al. Statistical determination of the optimal subthalamic nucleus stimulation site in patients with Parkinson disease. J Neurosurg 2007;106:101–10.
Guo T, Finnis KW, Parrent AG, Peters TM. Visualization and navigation system development and application for stereotactic deep-brain neurosurgeries. Comput Aided Surg 2006;11:231–9.
Haegelen C, Coupe P, Fonov V, Guizard N, Jannin P, Morandi X, Collins DL. Automated segmentation of basal ganglia and deep brain structures in MRI of Parkinson's Disease. Int J Comput Assist Radiol Surg, in press.
Hamani C, Saint-Cyr JA, Fraser J, Kaplitt M, Lozano AM. The subthalamic nucleus in the context of movement disorders. Brain 2003;127(1):4–20.
Hoehn M, Yahr M. Parkinsonism: onset, progression and mortality. Neurology 1967;17(5):427–42.
Houeto JL, Mesnage V, Mallet L, Pillon B, Gargiulo M, du Moncel ST, et al. Behavioural disorders, Parkinson's disease and subthalamic stimulation. J Neurol Neurosurg Psychiatry 2002;72:701–7.
Huebl J, Schoenecker T, Siegert S, Brücke C, Schneider GH, Kupsch A, et al. Modulation of subthalamic alpha activity to emotional stimuli correlates with depressive symptoms in Parkinson's disease. Mov Disord 2011;26:477–83.
Karachi C, Yelnik J, Tandé D, Tremblay L, Hirsch E, François C. The pallidosubthalamic projection: an anatomical substrate for nonmotor functions of the subthalamic nucleus in primates. Mov Disord 2005;20(2):172–80.
Khan MF, Mewes K, Gross RE, Skrinjar O. Assessment of brain shift related to deep brain stimulation surgery. Stereotact Funct Neurosurg 2008;86(1):44–53.
Kim YH, Kim HJ, Kim C, Kim DG, Jeon BS, Paek SH. Comparison of electrode location between immediate postoperative day and 6 months after bilateral subthalamic nucleus deep brain stimulation. Acta Neurochir (Wien) 2010;152(12):2037–45.
Klein A, Andersson J, Ardekani BA, Ashburner J, Avants B, Chiang MC, et al. Evaluation of 14 nonlinear deformation algorithms applied to human brain MRI registration. Neuroimage 2009;46(3):786–802.
Krack P, Pollak P, Limousin P, Hoffmann D, Xie J, Benazzouz A, et al. Subthalamic nucleus or internal pallidal stimulation in young onset Parkinson's disease. Brain 1998;121:451–7.
Krack P, Batir A, Van Blercom N, Chabardes S, Fraix V, Ardouin C, et al. Five-year follow-up of bilateral stimulation of the subthalamic nucleus in advanced Parkinson's disease. N Engl J Med 2003;349:1925–34.
Kühn AA, Hariz MI, Silberstein P, Tisch S, Kupsch A, Schneider GH, et al. Activation of the subthalamic region during emotional processing in Parkinson disease. Neurology 2005;65:707–13.
Lalys F, Haegelen C, Abadie A, Jannin P. Post-operative assessment in Deep Brain Stimulation based on multimodal images: registration workflow and validation. In: Medical imaging 2009: visualization, image-guided procedures, and modelling; 2009.
Lalys F, Haegelen C, Ferre JC, El-Ganaoui O, Jannin P. Construction and assessment of a 3T MRI brain template. Neuroimage 2011;49(1):345–54.
Lambert C, Zrinzo L, Nagy Z, Lutt A, Hariz M, Foltynie T, et al. Confirmation of functional zones within the human subthalamic nucleus: patterns of connectivity and sub-parcellation using diffusion weighted imaging. Neuroimage 2012;60(1):83–94.
Lang AE, Lozano AM. Parkinson's disease. N Engl J Med 1998;339(15):1044–53.
Langston JW, Widner H, Goetz CG, Brooks D, Fahn S, Freeman T, et al. Core assessment program for intracerebral transplantation (CAPIT). Mov Disord 1992;7(1):2–13.
Lanotte MM, Rizzone M, Bergamasco B, Faccani G, Melcarne A, Lopiano L. Deep Brain Stimulation of the subthalamic nucleus: anatomical, neurophysiological, and outcome correlations with the effects of stimulation. J Neurol Neurosurg Psychiatry 2002;72:53–8.
Lee JY, Kim JW, Lee JY, Lim YH, Kim C, Kim DG, et al. Is MRI a reliable tool to locate the electrode after deep brain stimulation surgery? Comparison study of CT and MRI for the localization of electrodes after DBS. Acta Neurochir (Wien) 2010;152(12):2029–36.
Lenglet C, Abosch A, Yacoub E, De Martino F, Sapiro S, Hare N. Comprehensive in vivo mapping of the human basal ganglia and thalamic connectome in individuals using 7T MRI. PLoS ONE 2012;7(1).
Lhommée E, Klinger H, Thobois S, Schmitt E, Ardouin C, Bichon A, et al. Subthalamic stimulation in Parkinson's disease: restoring the balance of motivated behaviours. Brain 2012;135:1463–77.
Maks CB, Butson CR, Walter BL, Vitek JL, McIntyre CC. Deep brain stimulation activation volumes and their association with neurophysiological mapping and therapeutic outcomes. J Neurol Neurosurg Psychiatry 2009;80(6):659–66.
Mallet L, Schüpbach M, N'Diaye K, Rémy P, Bardinet E, Czernecki V, et al. Stimulation of subterritories of the subthalamic nucleus reveals its role in the integration of the emotional and motor aspects of behavior. Proc Natl Acad Sci USA 2007;104:10661–6.
Mangin JF. Entropy minimization for automatic correction of intensity non uniformity. Hilton Head Island: IEEE Press; 2000, p. 162–169.
Mattis S. Dementia Rating scale. In: Professional manual. Odessa, FL: Psychological Assessment resources; 1988.
Medtronic. MRI guidelines for medtronic deep brain stimulation systems, 2006.
Mehri M, Lalys F, Maumet C, Haegelen C, Jannin P. Analysis of electrodes placement and deformations in deep brain stimulation. SPIE Med Imaging 2012:8316–32.
Nowinski WL, Belov D, Benabid AL. An algorithm for rapid calculation of a probabilistic functional atlas of subcortical structures from electrophysiological data collected during functional neurosurgery procedures. Neuroimage 2003;18:143–55.
Nowinski WL, Belov D, Pollak P, Banabid AL. Statistical analysis of 168 bilateral subthalamic nucleus implantations by means of the probabilistic functional atlas. Neurosurgery 2005;57(4):319–30.
Nowinski WL, Thirunavuukarasuu A, Liu J, Benabid AL. Correlation between the anatomical and functional human subthalamic nucleus. Stereotact Funct Neurosurg 2007;85:88–93.
Pallavaram S, Dawant BM, Remple M, Neimat JS, Kao C, Konrad PE, et al. Effect of brain shift on the creation of functional atlases for deep brain stimulation surgery. Int J Comput Assist Radiol Surg 2009;5(3):221–8.
Pallavaram S, D'Haese PF, Kao C, Yu H, Remple M, Neimat JS, et al. A new method for creating electrophysiological maps for DBS surgery and their application to surgical guidance. Med Image Comput Comput Assist Interv 2008:670–7.
Parsons TD, Rogers SA, Braayen AJ, Woods SP, Troster AI. Cognitive sequelae of subthalamic nucleus deep brain stimulation in Parkinson's disease: a meta-analysis. Lancet Neurol 2006;5:578–88.
Pollo C, Vingerhoets F, Pralong E, Ghika J, Maeder P, Meuli R, et al. Localisation of electrodes in the subthalamic nucleus on magnetic resonance imaging. J Neurosurg 2007;106:36–44.

Please cite this article in press as: Lalys F, et al. Anatomo-clinical atlases correlate clinical data and electrode contact coordinates: Application to subthalamic deep brain stimulation. J Neurosci Methods (2012), http://dx.doi.org/10.1016/j.jneumeth.2012.11.002

Psychological assessment resources. Computerized Wisconsin Card Sort Task Version 4 (WCST), 2003.
Rodriguez-Oroz MC, Rodriguez M, Guridi J, Mewes K, Chockkman V, Vitek J, et al. The subthalamic nucleus in parkinson's disease: somatotopic organization and physiological. Brain 2001;124(9):1777–90.
Reitan RM. Validity of the Trail Making test as an indicator of organic brain damage. Percept Mot Skills 1958;8:271–6.
Saint-Cyr JA, Trépanier LL, Kumar R, Lozano AM, Lang AE. Neuropsychological consequences of chronic stimulation of the subthalamic nucleus in Parkinson's disease. Brain 2000;123:2091–108.
Saint-Cyr JA, Hoque T, Pereira LC, Dostrovsky JO, Hutchison WD, Mikulis DJ, et al. Localization of clinically effective stimulating electrodes in the human subthalamic nucleus on magnetic resonance imaging. J Neurosurg 2002;97(5):1152–66.
Schaltenbrand G, Wahren W. Atlas for stereotaxy of the human brain. Stuttgart, Germany: Thieme; 1977.
Schwab RS, England AC. Projection techniques for evaluating surgery in Parkinson's disease. In: Third symp on Parkinson's disease; 1968, p. 152–157.
Stancanello J, Muacevic A, Sebastiano F, Modugno N, Cerveri P, Ferrigno G, et al. 3T MRI evaluation of the accuracy of atlas-based subthalamic nucleus identification. Med Phys 2008;35(7):3069–77.
Stroop JR. Studies of interference in serial verbal reactions. J Exp Psychol 1935;18:643–62.
Talairach J, Tournoux P. Co-planar stereotaxic atlas of the human brain. Stuttgart, Germany: Thieme; 1988.
Temel Y, Kessels A, Tan S, Topdag A, Boon P, Visser-Vandewalle V. Behavioural changes after bilateral subthalamic stimulation in advanced Parkinson disease: a systematic review. Parkinsonism Relat Disord 2006;12:265–72.
Theodosopoulos PV, Marks WJ, Christine C, Starr PA. Locations of movement-related cells in the human subthalamic nucleus in Parkinson's disease. Mov Disord 2003;18(7):791–8.
Troyer AK, Moscovitch M, Winocur G, Leach L, Freedman M. Clustering and switching on verbal fluency tests in Alzheimer's and Parkinson's disease. J Int Neuropsychol Soc 1998;4(2):137–43.
Volkmann J, Albanese A, Kulisevsky J, Tornqvist AL, Houeto JL, Pidoux B, et al. Long-term effects of pallidal or subthalamic deep brain stimulation on quality of life in Parkinson's disease. Mov Disord 2009;24:1154–61.
Witt K, Daniels C, Reiff J, Krack P, Volkmann J, Pinsker MO, et al. Neuropsychological and psychiatric changes after deep brain stimulation for Parkinson's disease: a randomized, multicentre study. Lancet Neurol 2008;7(7):605–14.
Yelnik J, Bardinet E, Dormont D, Malandain G, Ourselin S, Tandé D, et al. A three-dimensional, histological and deformable atlas of the human basal ganglia. I. Atlas construction based on immunohistochemical and MRI data. Neuroimage 2007;37:618–38.
York MK, Wilde EA, Simpson R, Jankovic J. Relationship between neuropsychological outcome and DBS surgical trajectory and electrode location. J Neurol Sci 2009;287(1,2):159–71.
Zaidel A, Spivak A, Grieb B, Bergman H, Israel Z. Subthalamic span of beta oscillations predicts deep brain stimulation efficacy for patients with Parkinson's disease. Brain 2010;133:2007–21.

Please cite this article in press as: Lalys F, et al. Anatomo-clinical atlases correlate clinical data and electrode contact coordinates: Application to subthalamic deep brain stimulation. J Neurosci Methods (2012), http://dx.doi.org/10.1016/j.jneumeth.2012.11.002